

# Prediction Technology and Its Application for Inter-Salt Shale Oil Reservoirs

An Liu\*

Shenzhen Water Planning & Design Institute Co., Ltd., Guangdong, Shenzhen 518000, China

\*Correspondence to: An Liu, Shenzhen Water Planning & Design Institute Co., Ltd., Guangdong, Shenzhen 518000, China, E-mail: [1154010507@qq.com](mailto:1154010507@qq.com)

**Abstract:** Shale oil is generally enriched in the pores or fractures of mudstone shale and is classified as an unconventional petroleum resource. According to statistics from the U.S. Energy Information Administration (EIA), the total global shale oil and gas resources have reached 936.835 billion barrels, with recoverable reserves of 61.847 billion barrels. The Jiangnan Basin is one of the main shale oil distribution basins in China. In the Qianjiang Sag, a set of salt series soil strata with a maximum thickness of 6000 meters has been deposited. Interbedded within the salt layers is a set of organic-rich fine-grained sedimentary rocks, with single layers up to 38 meters thick, which can act as both oil-generating and oil-storing layers. The shale oil resources between the salt layers in the Qianjiang Sag have great potential, with a cumulative oil production of 104,000 tons. Currently, conditions for capacity building have been preliminarily established, showing promising prospects for exploration and development.

This paper focuses on the extraction and analysis of seismic attributes for the target strata of the Qianjiang Formation in the Jiangnan region, specifically the 33x~342~41x objective layer interval. Representative post-stack geometric seismic attributes for fracture identification, such as curvature, coherence, and fracture likelihood attributes, are primarily selected. Preliminary reservoir prediction research is conducted, delineating potential locations of bedding fractures on planar maps<sup>[1]</sup>. These findings are combined with constrained sparse pulse seismic inversion results and lithology-based geostatistical seismic inversion results for a comprehensive analysis of the target reservoir interval. This dual approach serves to validate the accuracy of both shale reservoir prediction methods and to more precisely map the development of bedding fractures and other fractures. This work aims to determine the oil-bearing properties of the region, identify geological structures, and ultimately complete the prediction of inter-salt shale oil reservoir bedding fractures.

**Keywords:** shale oil; bedding fractures; reservoir prediction



© The Author(s) 2024. **Open Access** This article is licensed under a Creative Commons Attribution 4.0 International License (<https://creativecommons.org/licenses/by/4.0/>), which permits unrestricted use, sharing, adaptation, distribution and reproduction in any medium or format, for any purpose, even commercially, as long as you give appropriate credit to the original author(s) and the source, provide a link to the Creative Commons license, and indicate if changes were made.

## 1. Post-Stack Geometric Seismic Attribute Extraction and Application

### 1.1 Curvature Attributes

In mathematics, curvature is a parameter that measures the degree of bending of a curve<sup>[2]</sup>. It is defined through differentiation as the rate of change of the tangential angle concerning the arc length at a specific point on the curve. The greater the curvature, the higher the degree of bending. In geophysical exploration, curvature can be represented as the second spatial derivative of the seismic reflection axis. To calculate the curvature at a specific point, a local quadratic surface fit based on the least squares method is applied to that point and its neighboring grid points. The fitting surface characteristic parameters can be represented by a series of quadratic equations. Combining these parameters yields different curvature measures. The spatial curvature characteristic method uses this technique to characterize the distribution state of geological bodies in different spaces, facilitating the determination of the geometric structures of faults, fractures, and folds.

#### 1.1.1 Mean Curvature

Mean curvature  $K_m$  is the average value of the principal curvatures (orthogonal curvatures) at a given point on a surface and is a constant value.

$$K_m = \frac{K_{\max} + K_{\min}}{2}$$

where  $K_{\max}$  is the maximum curvature, and  $K_{\min}$  is the minimum curvature.

#### 1.1.2 Gaussian Curvature

Gaussian curvature, also known as total curvature, is used to calculate the maximum and minimum curvatures along with the mean curvature. The Gaussian curvature of a surface remains unchanged under isometric deformations.

$$K_g = K_{\max} \cdot K_{\min}$$

where  $K_{\max}$  is the maximum curvature, and  $K_{\min}$  is the minimum curvature.

#### 1.1.3 Maximum and Minimum Curvature

At any given point on a time surface, there are infinitely many orthogonal curvatures. The curve with the maximum curvature at the intersection point is called the maximum curvature, and the orthogonal curvature to this is the minimum curvature. Positive

values of maximum curvature represent the upthrown side of a fault, while negative values represent the downthrown side. The minimum curvature behaves inversely.

$$K_{\max} = K_m + \sqrt{K_m^2 - K_g}$$

$$K_{\min} = K_m - \sqrt{K_m^2 - K_g}$$

where  $K_m$  is the mean curvature, and  $K_g$  is the Gaussian curvature.

#### 1.1.4 Maximum Positive Curvature and Minimum Negative Curvature

The maximum positive curvature is the largest positive value of the normal curvature, while the minimum negative curvature is the smallest negative value. Together, they can be used to determine the geological structures of the subsurface formations<sup>[3]</sup>.

#### 1.1.5 Dip Curvature and Strike Curvature

Dip curvature is the curvature obtained along the direction of maximum dip, describing the rate of change in curvature along this direction. Strike curvature, obtained perpendicular to dip curvature along the strike direction, is used in combination with dip curvature for geomorphological analysis.

### 1.2 Coherence Attributes

Tectonic movements over many years cause the formation of faults, fractures, and various other types of geological anomalies within the strata. These anomalies result in unevenly inclined lithological characteristics on the surface, altering the information within adjacent seismic traces. Coherence technology uses the variation in the coherence values of seismic signals to characterize the horizontal heterogeneity of strata structures and lithologies. This allows for the study of the spatial distribution patterns of geological structures such as faults and micro-faults, providing a spatial representation of the entire lithological structure.

In this study, the third-generation coherence technology based on eigenstructure analysis is used to extract seismic coherence attributes. Compared to the first-generation coherence technology, which uses cross-correlation coherence stacking, and the second-generation coherence technology, which uses similarity coherence, the third-generation coherence technology employs eigenvalue decomposition. This algorithm,

utilizing principal component analysis, is slower but more stable, offering better fidelity, higher resolution, and a clearer and more detailed presentation of geological features.

Assuming there are  $J$  traces in the analysis window with coordinates  $(x_i, y_i)$ , centered on a time aperture  $T = n\Delta t$ , the covariance matrix is calculated for  $2m+1$  sample points along pairs of apparent dips and azimuths  $(p, q)$ .

$$C = \sum_{m=n-M}^{n+M} \begin{pmatrix} u_{1m}u_{1m} & \cdots & u_{1m}u_{Jm} \\ \vdots & \ddots & \vdots \\ u_{Jm}u_{1m} & \cdots & u_{Jm}u_{Jm} \end{pmatrix}$$

$$C_3(p, q) = \frac{\lambda_i}{\sum_{j=1}^J \lambda_j}$$

Let  $\lambda_i$  be the eigenvalues of the covariance matrix, where  $\lambda_i$  is the largest. The coherence value can then be defined as  $C_3$ , where setting  $(p, q)$  to zero provides the coherence value for the algorithm.

The coherence value primarily depends on the spatial  $J$  and temporal apertures  $T$ : (1) The greater the number of traces involved in the coherence calculation, the larger the averaging effect between sampling points, effectively suppressing noise. In this case, coherence primarily highlights the lateral variation in seismic coherence. With fewer traces involved, the averaging effect is smaller, increasing resolution but making the result more susceptible to noise interference. (2) A longer temporal aperture can suppress noise within the coherence cube, emphasizing the continuity of strata. In contrast, a shorter temporal aperture can better highlight the characteristics of fractured strata and low-angle faults.

### 1.3 Fault Likelihood Attribute

Fault structures significantly impact the extraction of oil and gas reservoirs. High-precision fault identification and interpretation are crucial aspects of oil and gas field exploration and development. After extracting and analyzing curvature and coherence attributes, the introduction of fault likelihood attributes can precisely delineate the boundaries of fault structures. This enhances the accuracy of stratigraphic interpretation and objectively maps the regions where faults are present.

The calculation of fault likelihood attributes is

based on seismic similarity, representing the degree of "maximum likelihood" of the presence of faults. The principle is derived from the analysis of seismic image similarity. Generally, the expression for calculating the fault likelihood attribute is as follows:

$$F = 1 - \text{Semblance}^8$$

Where  $F$  is the fault likelihood attribute, and *Semblance* represents the seismic coherence attribute. The fault likelihood attribute uses the difference between the eighth power of the coherence attribute value and 1. This effectively highlights fault anomalies in the imaging. A larger *Semblance* attribute value corresponds to a smaller likelihood attribute value, indicating a lower probability of fault development and more continuous adjacent seismic traces. Conversely, a smaller *Semblance* attribute value corresponds to a larger fault likelihood attribute value, indicating a higher probability of fault development.

## 2 Reservoir Description Technology and Application Based on Lithologic Inversion

### 2.1 Constrained Sparse Spike Inversion

The Constrained Sparse Spike Inversion (CSSI) method is currently the most commonly used technique in seismic inversion work. Initially, the acoustic time difference curve and density curve from the original logging data are used to calculate the well's impedance curve. A geological framework is then established, through which an initial impedance model is generated by interpolation. This initial model, along with the trends from the impedance model and logging curves, is used to constrain the inversion results and obtain the reflection coefficient sequence of the subsurface formations. A high-quality constrained sparse spike inversion achieves two main objectives: it can depict the lateral variation trends of the subsurface formation impedance, and it provides essential data such as signal-to-noise ratio and low-frequency models for subsequent lithology-based geostatistical inversion. Additionally, it allows for comparison and analysis of differences between the two inversion methods by integrating results from the lithology-based geostatistical inversion.

In the constrained sparse spike inversion, the

objective function for the reflection sequence with the minimum number of spikes is given by:

$$J = \sum |r_i|^p + \lambda^q \sum (d_i - s_i)^q + \alpha^2 \sum (t_i - z_i)^2$$

where  $J$  represents the objective function,  $r_i$  is the estimated reflection coefficient sequence,  $d_i$  is the original seismic data,  $s_i$  is the synthetic seismic record,  $\lambda$  is the weight coefficient for the residual between the synthetic seismic record and the actual seismic data,  $t_i$  represents the trend of the well impedance curve,  $z_i$  is the control parameter within the hard constraint range centered on the well impedance trend, and  $\alpha$  denotes the degree to which the well impedance trend constrains the inversion result. Generally, the values are  $\alpha = 1, p = 1, q = 2$ .

### 2.2 Geostatistical Inversion

Constrained sparse spike inversion is a direct seismic trace inversion method based on actual seismic data. The accuracy of its results largely depends on the quality of the seismic data. Since the frequency bandwidth of actual seismic data typically ranges from a few tens to several tens of Hertz, the vertical

resolution of the results from constrained sparse spike inversion is not guaranteed, making it difficult to accurately identify reservoirs. To address this limitation, geostatistical inversion is introduced for reservoir identification.

Geostatistical inversion is based on geostatistics and stochastic simulation. Initially, a statistical analysis of the well data within the work area is conducted. This analysis is then applied to the stochastic simulation process to generate a wave impedance data volume. The differences between the synthetic seismic records and the actual seismic data are analyzed, and the stochastic simulation process is constrained accordingly. This process is repeated until the simulation results meet the preset conditions. The final simulation result is considered the inversion result. Geostatistical inversion leverages the continuity of seismic data and the high vertical resolution of well log data, combining the advantages of both data types. This approach allows for accurate reservoir prediction, particularly for thin reservoirs.

### 2.3 Inversion Result Analysis

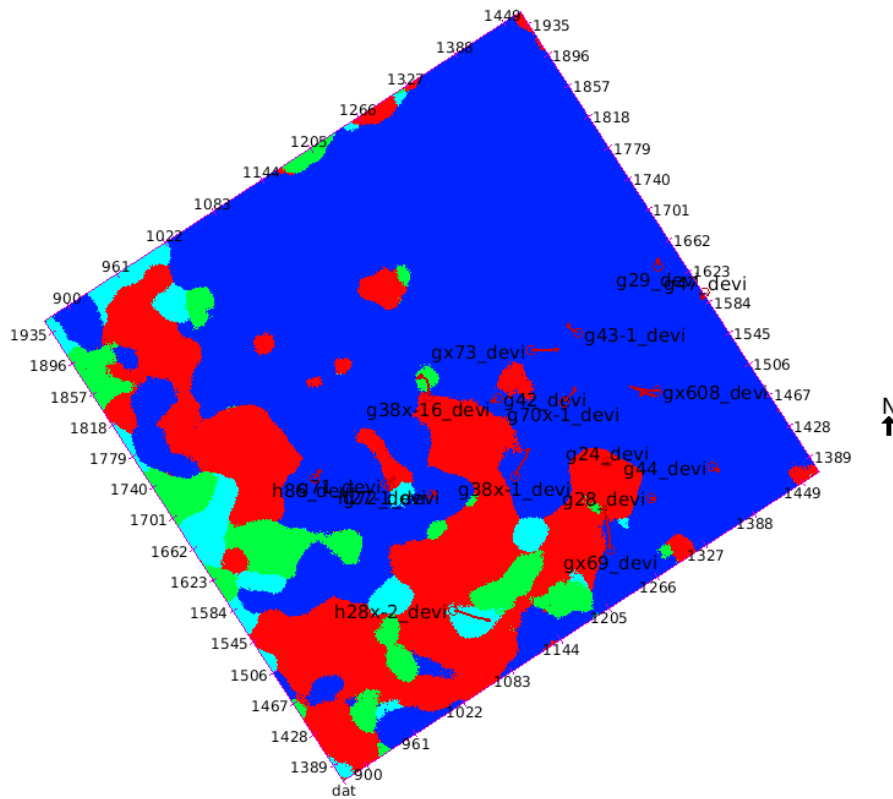


Figure 1: Lithology Body Distribution Map

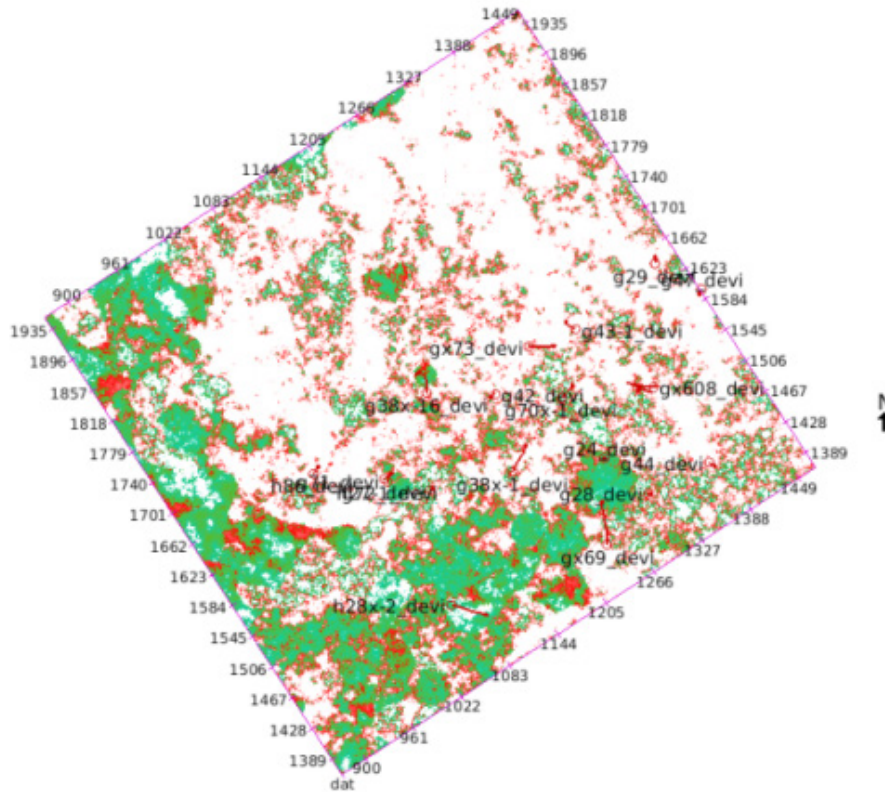


Figure 2: Wave Impedance Distribution Map

Project the lithology body obtained from geostatistical inversion onto a plane and analyze it. There are three main types of lithologies in the work area: salt rock, carbonaceous dolomite, and mudstone. According to previous literature research, fractures (bedding fractures) primarily develop in carbonaceous dolomite and are not present in mudstone and salt rock. In the figure, the red blocks represent areas where bedding fractures are developed, distributed in the southeastern, south-central, and southwestern parts of the work area. Next, project the P-wave impedance body obtained from geostatistical inversion onto a plane to create a wave impedance distribution map. By analyzing the lithology body distribution map and the wave impedance distribution map together, we find that the impedance at productive well locations is concentrated in the range of 7500~10000g/cc\*m/s. This corresponds to the areas with moderate P-wave impedance values, represented by the red and green parts of the map, which can be considered favorable reservoir zones for the 33x to 41x target intervals in the work area.

### Conclusion

Combining the analysis results of post-stack seismic attributes with the planar distribution maps of lithology bodies and wave impedance obtained from geostatistical inversion, we can identify areas with well-developed bedding fractures in the 33x to 41x target intervals. These areas are mainly concentrated in the southeastern, southwestern, and south-central parts of the work area, indicating a high potential for the presence of shale oil in these regions.

During comprehensive seismic attribute analysis, it is often found that a single attribute may not precisely reflect detailed structures such as faults or fractures. By using dual or multiple seismic attribute fusion techniques, where two or more different seismic attributes are combined, we can more accurately determine the scale and location of fractures, significantly enhancing the detailed depiction of fractures.

Compared to constrained sparse spike inversion, geostatistical inversion employs statistical principles in deterministic inversion, effectively combining the high

vertical resolution of well log data with the high lateral resolution of seismic data. In terms of the accuracy required for reservoir prediction, geostatistical inversion overcomes the low vertical resolution issue of constrained sparse spike inversion. Thus, the inversion results from geostatistical inversion are more detailed and complete than those from constrained sparse spike inversion.

## References

- [1] Fang Yuan, Zhang Wanyi, Ma Su, et al. Global distribution and development status of shale oil resources [J]. *Mineral Conservation and Utilization*, 2019, 39(05): 126-134.
- [2] Hou Xinye, Li Xin. Application of multi-attribute fusion technology in seismic identification of tight sandstone gas [C]. *Proceedings of the 2021 Geophysical Technology Symposium of the Chinese Petroleum Society*, 2021: 1340-1343.
- [3] Guo Jianqing. Application of seismic inversion technology in the identification and prediction of carbonate reservoirs [J]. *Inner Mongolia Petrochemical*, 2020, 46(02): 82-86.